Global polarization of Λ and $\overline{\Lambda}$ hyperons in Pb Pb collisions at $\sqrt{s}$ 2.76 and 5.02 TeV

S. Acharya *et al.*[*]
(ALICE Collaboration)

The global polarization of the Λ and $\overline{\Lambda}$ hyperons is measured for Pb-Pb collisions at $\sqrt{s_{NN}} = 2.76$ and 5.02 TeV recorded with the ALICE at the Large Hadron Collider (LHC). The results are reported differentially as a function of collision centrality and hyperon's transverse momentum (p_T) for the range of centrality 5–50 , $0.5 < p_T < 5$ GeV/c, and rapidity $|y| < 0.5$. The hyperon global polarization averaged for Pb-Pb collisions at $\sqrt{s_{NN}} = 2.76$ and 5.02 TeV is found to be consistent with zero, $\langle P_H \rangle( ) \approx 0.01 \pm 0.06$ (stat.) ± 0.03 (syst.) in the collision centrality range 15–50 , where the largest signal is expected. The results are compatible with expectations based on an extrapolation from measurements at lower collision energies at the Relativistic Heavy Ion Collider, hydrodynamical model calculations, and empirical estimates based on collision energy dependence of directed flow, all of which predict the global polarization values at LHC energies of the order of 0.01 .

I. INTRODUCTION

The system created in a noncentral nucleus-nucleus collision might retain a significant fraction of the large orbital angular momentum of the colliding nuclei. Due to the spin-orbit coupling, particles produced in such a collision can become globally polarized [1–4]. The global polarization is a phenomena when spins of all emitted final-state particles in a noncentral nucleus-nucleus collision are aligned along one preferential direction defined by the initial angular orbital momentum. Its measurement provides important information about the initial conditions and dynamics of the quark-gluon plasma (QGP), as well as the hadronization process [5–7]. The global polarization for a specific particle and corresponding antiparticle is expected to be very similar, or even identical, in a system with small or zero baryon chemical potential.

High-energy heavy-ion collisions are also characterized by ultrastrong magnetic fields [8,9], which on average are aligned with the direction of the angular momentum. While the peak values of the magnetic fields, which reach up to 10^{18} Gauss, can be estimated rather accurately [8,9], the time evolution, which depends on the QGP electric conductivity, is practically unknown. These fields can also contribute to the global polarization, but their action on particles and antiparticles is expected to be in an opposite direction. Thus the measurement of the splitting between particle and antiparticle global polarizations provides very valuable information about the QGP properties.

The measurements of the global polarization P_H for spin one half Λ ($\overline{\Lambda}$) strange hyperons are experimentally favorable because their spin direction can be reconstructed via their weak decay topology into proton (antiproton) and charged pion. Recently, the STAR Collaboration observed nonzero global polarization of Λ and $\overline{\Lambda}$ hyperons in Au-Au collisions, first for the Relativistic Heavy Ion Collider (RHIC) beam energy scan (BES) energies of $\sqrt{s_{NN}} = 7$–39 GeV and, later, with more data, at $\sqrt{s_{NN}} = 200$ GeV [10,11]. The magnitude of the observed polarization varies from a few to a fraction of a percent. While the P_H values for Λ and $\overline{\Lambda}$ agree within the experimental uncertainties, they are systematically higher for $\overline{\Lambda}$ than for Λ. Assuming that this difference originates due to the magnetic fields one estimates the field strength in units of elementary charge e to be $eB \sim 0.01 m_\pi^2$ [12].

The exact nature of the spin-orbit interaction leading to the global polarization is not known. It is unclear at what stage of the system evolution (the QGP, hadronization, or the hadronic rescattering) the polarization is acquired, neither the corresponding relaxation times are known. Most of the recent calculations of the global polarization assume complete thermal equilibrium and validity of the hydrodynamical description of the system [6,12–15]. They relate the particle polarization to the system's thermal vorticity at the hadronization time. In a nonrelativistic limit, assuming complete thermal equilibrium, the polarization of the particles can be evaluated as $\zeta = \langle \mathbf{s} \rangle / s = (s + 1) /(3T)$, where s is the particle's spin, T is the system temperature, $= (1/2)(\nabla \times \mathbf{v})$ is a nonrelativistic vorticity, and $\mathbf{v}$ is the local fluid velocity [12].

The global polarization is determined by the average vorticity component perpendicular to the collision reaction plane, which is spanned by the beam direction and the impact parameter vector. The global polarization measurements with the produced particle provide important information on both the nature of the spin-orbit interaction and the profile of velocity fields of the expanding system. Both the magnitude and the

---

direction of the vorticity can strongly vary within the system [16]. In particular, a significant component along the beam direction can be acquired due to the transverse anisotropic flow [16,17].

The vorticity of the system, especially its component along the system's orbital momentum, is directly related to the asymmetries in the initial velocity fields. This links the vorticity with the directed flow v_1, which is also strongly dependent on those asymmetries. The v_1 is defined by the first Fourier moment $v_1 = \langle \cos(\varphi - \Psi_{RP}) \rangle$ of the produced particle's azimuthal asymmetry relative to the collision reaction plane angle Ψ_{RP}. Hydrodynamic simulations show that the orbital angular momentum stored in the system and the directed flow of charged particles are almost directly proportional to each other [5]. This allows for an empirical estimate of the collision energy dependence of the global polarization [16]. The STAR results for the directed flow [18,19] and the hyperon global polarization [10,11] from the BES program show that the slopes of v_1 at midrapidity $(dv_1/d\eta)$ for charged hadrons (pions) and the hyperon polarization are indeed strongly correlated. The charged-particle directed flow in Pb-Pb collisions at $\sqrt{s_{NN}} = 2.76$ TeV is about three times smaller [20] than at the top RHIC energy of 200 GeV. This suggest that the global polarization at the Large Haron Collider (LHC) energies should be also about three times smaller than at RHIC (around ~ 0.08) and decreasing from $\sqrt{s_{NN}} = 2.76$ to 5.02 TeV by about ~ 30 [21]. Even smaller polarization values at the LHC are expected when the directed flow is seen as a combination of the two effects: the tilt of the source in the longitudinal direction and the dipole flow originating from the asymmetry in the initial energy density distributions [22]. Taking into account that only the contribution to the directed flow from the tilted source is related to the vorticity and that its contribution relative to the dipole flow decreases with the collision energy [22], one arrives to an estimate for the global polarization at the LHC energies of the order of ~ 0.04 .

In this paper, the measurements of the global polarization of the Λ and $\overline{\Lambda}$ hyperons in Pb-Pb collisions at $\sqrt{s_{NN}} = 2.76$ and 5.02 TeV recorded with ALICE at the LHC are reported. The paper is organized as follows. In Sec. II the analysis details are presented, and the global polarization observable is introduced, as well as the measurement technique. The various sources of systematic uncertainties are discussed in Sec. III. The results for the Λ and $\overline{\Lambda}$ global polarization at two collision energies as a function of the hyperon transverse momentum and collision centrality are presented in Sec. IV.

II. DATA ANALYSIS

A. The observable

In this measurement, Λ and $\overline{\Lambda}$ hyperons are reconstructed through their weak decay topologies $\Lambda \to p + \pi^-$ and $\overline{\Lambda} \to \bar{p} + \pi^+$ (64 branching ratio). The global polarization of the hyperons is determined from the angular distributions of their decay (anti-)protons. In the hyperon rest frame, the (anti-)proton angular probability distribution, $dw/d\boldsymbol{n}_p^*$, is given by

$$\frac{dw}{d\boldsymbol{n}_p^*} = 1 + \alpha_H \, \boldsymbol{\zeta}_H \cdot \boldsymbol{n}_p^*, \tag{1}$$

where $\boldsymbol{n}_p^*$ is the unit vector of the (anti-)proton direction. The same absolute value from [23] for the hyperon decay parameter $\alpha_H = 0.642 \pm 0.013$, positive for Λ and negative for $\overline{\Lambda}$, is used. Recent measurement by the BESIII Collaboration [24] extracted a new values for $\alpha_\Lambda = 0.750 \pm 0.010$ and $\alpha_{\bar{\Lambda}} = -0.758 \pm 0.012$, which are about 17 larger than in Ref. [23]. Given the statistical and systematical uncertainties of the results reported below for the hyperon global polarization the new values for α_H will not change the conclusions of this paper but they should be considered for future hight precision measurements. The polarization vector $\boldsymbol{\zeta}_H$ in Eq. (1), which is satisfying condition $|\boldsymbol{\zeta}_H|$ 1, can be measured experimentally as [25]

$$\boldsymbol{\zeta}_H = \frac{3}{\alpha_H} \langle \boldsymbol{n}_p^* \rangle, \tag{2}$$

where the brackets $\langle \dots \rangle$ denote an event-by-event averaging over all hyperon decays.

The polarization vector $\boldsymbol{\zeta}_H$ generally depends on the hyperon kinematics, namely the transverse momentum p_T, rapidity y, and its azimuthal angle with respect to the reaction plane, $\varphi - \Psi_{RP}$, as well as the collision centrality. The global polarization reported in this paper is determined by the component of the polarization vector perpendicular to the reaction plane. The magnitude P_H of the global polarization can be measured by averaging a corresponding projection of the $\boldsymbol{n}_p^*$ vector, which in the laboratory coordinate system is given by $n_{p\perp RP}^* = \sin\theta_p^* \sin(\varphi_p^* - \Psi_{RP})$. Here θ_p^* (φ_p^*) is the polar angle with respect to the collision axis (azimuthal angle) of the (anti-)proton direction in the hyperon rest frame. Substituting $n_{p\perp RP}^*$ into Eq. (2) and assuming an ideal detector acceptance, an average over the θ_p^* yields

$$P_H = \frac{8}{\pi \alpha_H} \langle \sin(\varphi_p^* - \Psi_{RP}) \rangle. \tag{3}$$

Here the brackets $\langle \dots \rangle$ imply averaging over individual hyperons in all events. The polarization is defined to be positive if the hyperon spin has a positive component along the system's angular momentum—the same convention as employed in Ref. [10]. The detector acceptance effects are treated in this work as systematic uncertainty and discussed in Sec. III.

A significant fraction of Λ and $\overline{\Lambda}$ hyperons originates from decay of heavier particles. Existing estimates [6,12,13] of the feed-down effect on the hyperon global polarization measurements, based on the assumption of thermal equilibrium and the particle yields from the statistical model [26], suggest that the primary Λ and $\overline{\Lambda}$ polarization should be by about 15–20 larger than what is measured at RHIC. Taking into account that feed-down effects are expected to be small compared to other uncertainties in the current analysis, no correction to the data has been applied.

B. Measurement technique

The main components of the ALICE detector system [27,28] used for this measurement are the Time Projection Chamber (TPC) [29], the silicon detectors of the Inner Tracking System (ITS) [30] and the two neutron Zero-Degree Calorimeters (ZDC) [31]. The analyzed data samples were

recorded by ALICE in 2010 and 2011 for Pb-Pb collisions at $\sqrt{s_{NN}} = 2.76$ TeV, and in 2015 for collisions at $\sqrt{s_{NN}} = 5.02$ TeV.

During the data taking, the trigger required a hit in a pair of V0 detectors [32]. In 2010 and 2011, events with only one V0 hit and at least two hits in the outer layer of the Silicon Pixel Detector (SPD) were accepted as well. Contamination from beam-induced background was removed offline, as discussed in Refs. [33,34]. The events with poor correlation between multiplicities in V0, ITS, and TPC detectors were rejected. The analysis was restricted to the events with the primary vertex along the beam direction, V_z, within ± 10 cm from the nominal center of the TPC. This yielded for all collision centralities approximately 49 (75) million of Pb-Pb collisions at $\sqrt{s_{NN}} = 2.76$ (5.02) TeV. The collision centrality was determined using the energy deposition in the V0 detectors [35].

The reaction plane angle Ψ_{RP} was estimated using the spectator plane angle Ψ_{SP}, characterizing the deflection direction of the spectator neutrons. The spectator deflections at positive and negative rapidity were reconstructed with a pair of neutron ZDC detectors located 114 m away from the interaction point. The Ψ_{SP} angle was evaluated separately for the two detectors using the transverse profile of the spectator energy distribution provided by the 2×2 segmentation of the ZDCs. For this, a pair of two-dimensional vectors $\mathbf{Q}^{t,p}$ were constructed for two ZDCs following the procedure described in Ref. [20]:

$$\mathbf{Q}^{t,p} \equiv \left(Q_x^{t,p}, Q_y^{t,p}\right) = \sum_{i=1}^{4} \mathbf{n}_i E_i^{t,p} \Big/ \sum_{i=1}^{4} E_i^{t,p}, \qquad (4)$$

where indices p and t denote the ZDC on the projectile ($\eta > 0$) and target ($\eta < 0$) side of the interaction point, respectively; E_i is the measured signal and $\mathbf{n}_i = (x_i, y_i)$ are the coordinates of the ith ZDC segment. The event averaged $\langle \mathbf{Q}^{t,p} \rangle$ revealed a strong dependence on the collision centrality as well as on the three collision vertex coordinates, which is imposed by the offset of the LHC beam transverse spot positions relative to the nominal center of the ZDCs. Moreover, the $\langle \mathbf{Q}^{t,p} \rangle$ demonstrated a strong time dependence in some of the 2015 runs. To compensate for these variations an event-by-event recentering correction [36] was applied as a function of collision centrality, three components of the collision vertex position, and beam-time variation,

$$\mathbf{Q}' = \mathbf{Q} - \langle \mathbf{Q} \rangle. \qquad (5)$$

Additionally to the procedure described in Ref. [20], the width of the $\mathbf{Q}'$ distributions was equalized as a function of centrality, which together with Eq. (5) resulted in an overall **Q**-vector correction,

$$Q_x'' = \frac{Q_x' - \langle Q_x \rangle}{\langle Q_x'^2 \rangle}, \quad Q_y'' = \frac{Q_y' - \langle Q_y \rangle}{\langle Q_y'^2 \rangle}. \qquad (6)$$

The width equalization, up to 20 , turned out to be particularly useful for the 2015 data sample, where one of the two neutron ZDC detectors lost signal from one of its four channels.
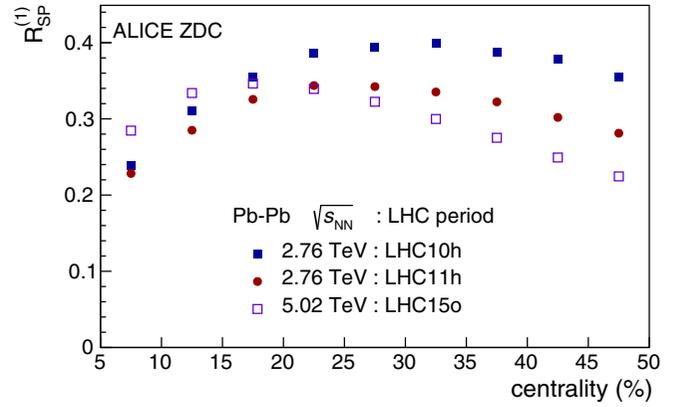

FIG. 1. The correction $R_{SP}^{(1)}$ for finite resolution of the spectator plane angle Ψ_{SP} as a function of collision centrality for three data sets used in the analysis. Only statistical uncertainties, which are smaller than a symbol size, are shown.

The Ψ_{SP} angle estimated from each ZDC is then given by the direction of the corrected $\mathbf{Q}''$ vector,

$$\mathbf{Q}'' = |\mathbf{Q}''| \exp\{i\Psi_{SP}\}. \qquad (7)$$

To account for a finite resolution of the spectator plane angle Ψ_{SP}, a correction $R_{SP}^{(1)}$ is introduce in the Eq. (3) following the method described in Ref. [25]:

$$P_H = \frac{8}{\pi \alpha_H} \frac{\langle \sin(\ _p^* - \Psi_{SP}) \rangle}{R_{SP}^{(1)}}. \qquad (8)$$

The polarization values obtained with Eq. (8) for each of the two ZDC detectors were found to be similar within the statistical uncertainties and were combined.

The correction $R_{SP}^{(1)}$ was extracted from correlations between **Q**-vector angles from different ALICE detectors following the technique described in Ref. [37]. Figure 1 presents the $R_{SP}^{(1)}$ as a function of collision centrality for different data sets. The most central (0–5) collisions are excluded from the analysis, because the small number of spectators does not allow for reliable estimation of the spectator deflection with the ZDCs. During the Pb-Pb data taking in 2011 ($\sqrt{s_{NN}} = 2.76$ TeV) and 2015 ($\sqrt{s_{NN}} = 5.02$ TeV), the beams were collided at a nonzero vertical crossing angle [28]. This resulted in a partial screening of the spectator neutrons by the LHC tertiary collimators [38] and in a degradation of the spectator plane resolution. The V0s, TPC, and two forward multiplicity detectors (FMD) [39] were used to estimate a possible uncertainties in $R_{SP}^{(1)}$ extraction for the two ZDC detectors. In all data samples, these uncertainties turned out to be at a level of several percent.

The Λ and $\overline{\Lambda}$ hyperons were reconstructed via their weak decay topology following the method and selection criteria described in Refs. [28,40]. Charged daughter tracks from hyperon decay were required to have the pseudorapidity $|\eta| < 0.9$ and at least 70 space points in the TPC. The pion and (anti-)proton particle type assignments were based on the track charge and specific energy loss (dE/dx) measured in the TPC. The daughter tracks were paired to form Λ and $\overline{\Lambda}$
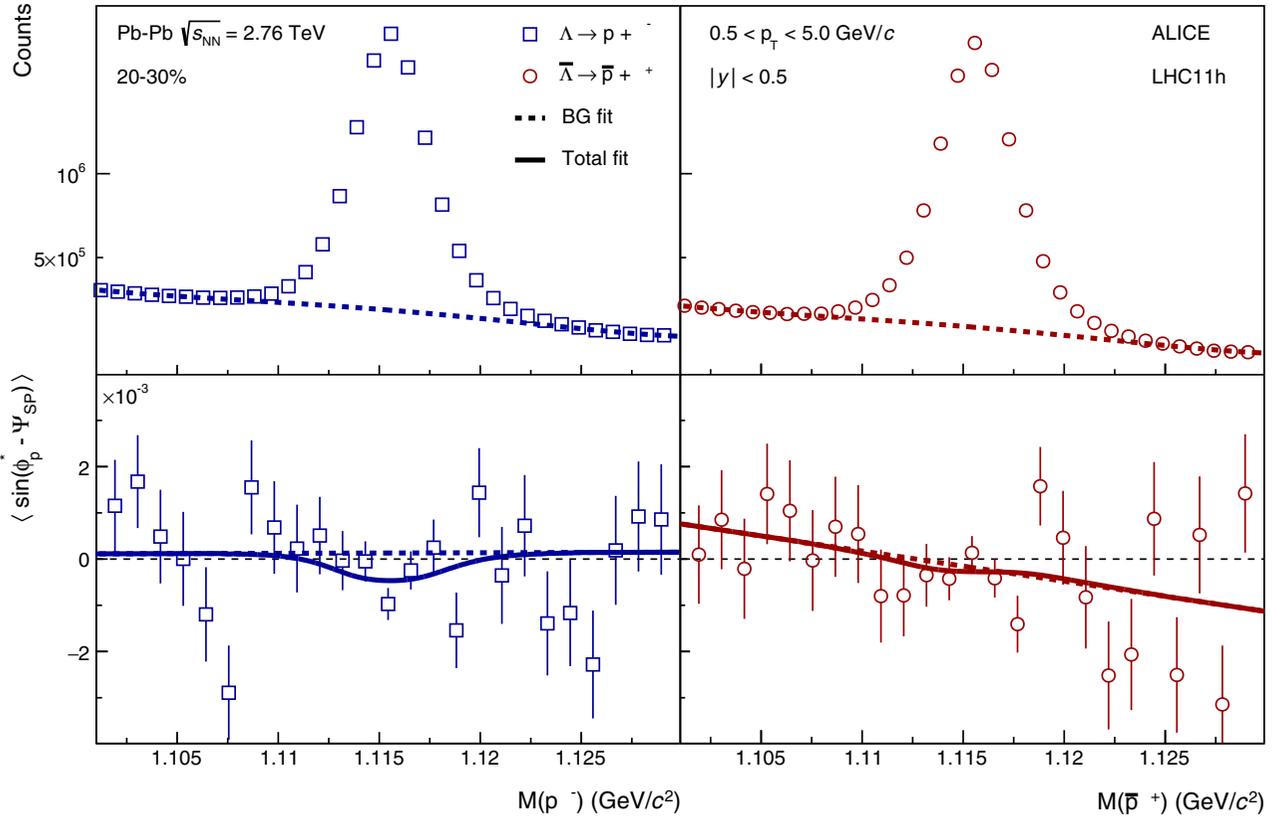
FIG. 2. Top panels: Invariant mass distributions of Λ (left) and $\overline{\Lambda}$ (right) candidates for 20–30 centrality range in Pb-Pb collisions at $\sqrt{s_{NN}} = 2.76$ TeV using data collected during the LHC operation in 2011. Dashed lines show the result of the fit for $N_{\mathrm{BG}}(M_{\mathrm{inv}})$ in Eq. (10). Bottom panels: Global polarization extraction via fit to $\langle \sin(\phi_p^* - \Psi_{\mathrm{SP}}) \rangle$ as a function of the invariant mass, with Ψ_{SP} reconstructed with the ZDC on the target ($\eta < 0$) side. Dashed and solid lines show $L_{\mathrm{BG}}(M_{\mathrm{inv}})$ and the combined fit with Eq. (9). See text for more details.

candidates. The candidates were required to have transverse momentum $p_T > 0.5$ GeV/c, rapidity $|y| < 0.5$, and the momentum vector pointing back to the primary collision vertex within a cone of opening angle less than 0.1 (0.08) radians for Pb-Pb collisions at $\sqrt{s_{NN}} = 2.76$ (5.02) TeV.

The hyperon global polarization P_H was extracted with the fit to the measured correlation $\langle \sin(\phi_p^* - \Psi_{\mathrm{SP}}) \rangle$ as a function of the Λ or $\overline{\Lambda}$ candidate invariant mass, M_{inv}:

$$\langle \sin(\phi_p^* - \Psi_{\mathrm{SP}}) \rangle (M_{\mathrm{inv}})$$
$$= [1 - f_{\mathrm{BG}}(M_{\mathrm{inv}})] \times S_H + f_{\mathrm{BG}}(M_{\mathrm{inv}}) \times L_{\mathrm{BG}}(M_{\mathrm{inv}}). \quad (9)$$

Here the constant S_H gives the numerator of Eq. (8) and $L(M_{\mathrm{inv}})$ is a linear parametrization of the background correlation as a function of M_{inv}. The background fraction $f_{\mathrm{BG}}(M_{\mathrm{inv}})$ was evaluated as

$$f_{\mathrm{BG}}(M_{\mathrm{inv}}) = \frac{N_{\mathrm{BG}}(M_{\mathrm{inv}})}{N_{\mathrm{tot}}(M_{\mathrm{inv}})}. \quad (10)$$

Here $N_{\mathrm{tot}}(M_{\mathrm{inv}})$ is the total measured yield of the Λ or $\overline{\Lambda}$ candidates. The $N_{\mathrm{BG}}(M_{\mathrm{inv}})$ is given by the fourth-order polynomial fit to the $N_{\mathrm{tot}}(M_{\mathrm{inv}})$ outside the Λ and $\overline{\Lambda}$ invariant mass peak range, $M_{\mathrm{inv}} < 1.107$ GeV/c^2 and $M_{\mathrm{inv}} > 1.125$ GeV/c^2.

The fitting procedure is illustrated in Fig. 2 for 20–30 centrality range in Pb-Pb collisions at $\sqrt{s_{NN}} = 2.76$ TeV using data collected during the LHC operation in 2011.

III. SYSTEMATIC UNCERTAINTIES

The considered sources of systematic uncertainties are summarized in Table I. The significance of a given systematical variation is determined following the procedure presented in Refs. [41].

The selection on the primary vertex position V_z was varied to ± 7 cm and ± 8 cm instead of the default ± 10 cm. The analysis was repeated with the collision centrality estimated with either ITS or TPC detectors (instead of the default V0 detector). Variations of the results when changing the event selection criteria described above and centrality estimators are found to be negligible and were not included into the total systematic uncertainty.

TABLE I. Systematic uncertainties in global polarization measurements for different data sets. Values reported as a fraction of the corresponding statistical uncertainty.

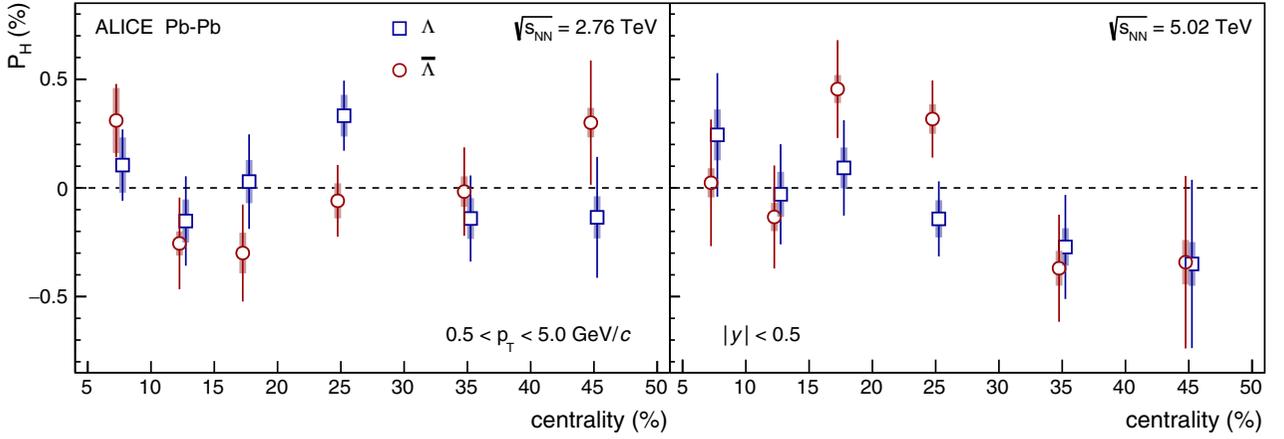| Data sample	Centrality	$\Lambda/\overline{\Lambda}$ candidate selection	Fitting procedure	Acceptance	$R_{\mathrm{SP}}^{(1)}$
2010	5−15	20	30	10	<2
	15−50		5		
2011	5−15	30	20	10	<2
	15−50		12		
2015	5−50	30	20	10	<4

FIG. 3. The global hyperon polarization as function of centrality for Pb-Pb collisions at $\sqrt{s_{NN}} = 2.76$ TeV (left) and 5.02 TeV (right). The systematic uncertainties are shown as shaded boxes. Points are slightly shifted along the horizontal axis for better visibility.

The following Λ and $\overline{\Lambda}$ candidate selection criteria were varied: the distance of closest approach to the primary vertex, decay daughter track selection via specific energy loss in the TPC, the distance of closest approach between the pair of the daughter tracks, and the criteria on the hyperon candidates momentum pointing angle to the primary vertex. The corresponding contribution from these variations to the total systematic uncertainty is about 20–30 of the statistical un-

certainty. The main contribution to the systematic uncertainty from the fitting procedure in Eq. (9) comes from a variation of the fit region.

In Eq. (8) a perfect acceptance of the hyperons and their decay daughters is assumed. In the case of an imperfect detector, there is a overall scale correction of the measured polarization as well as a possible admixture of higher-order harmonics in a Fourier decomposition of the $dN_{\Lambda/\overline{\Lambda}}/d(\phi_p^* - \Psi_{RP})$
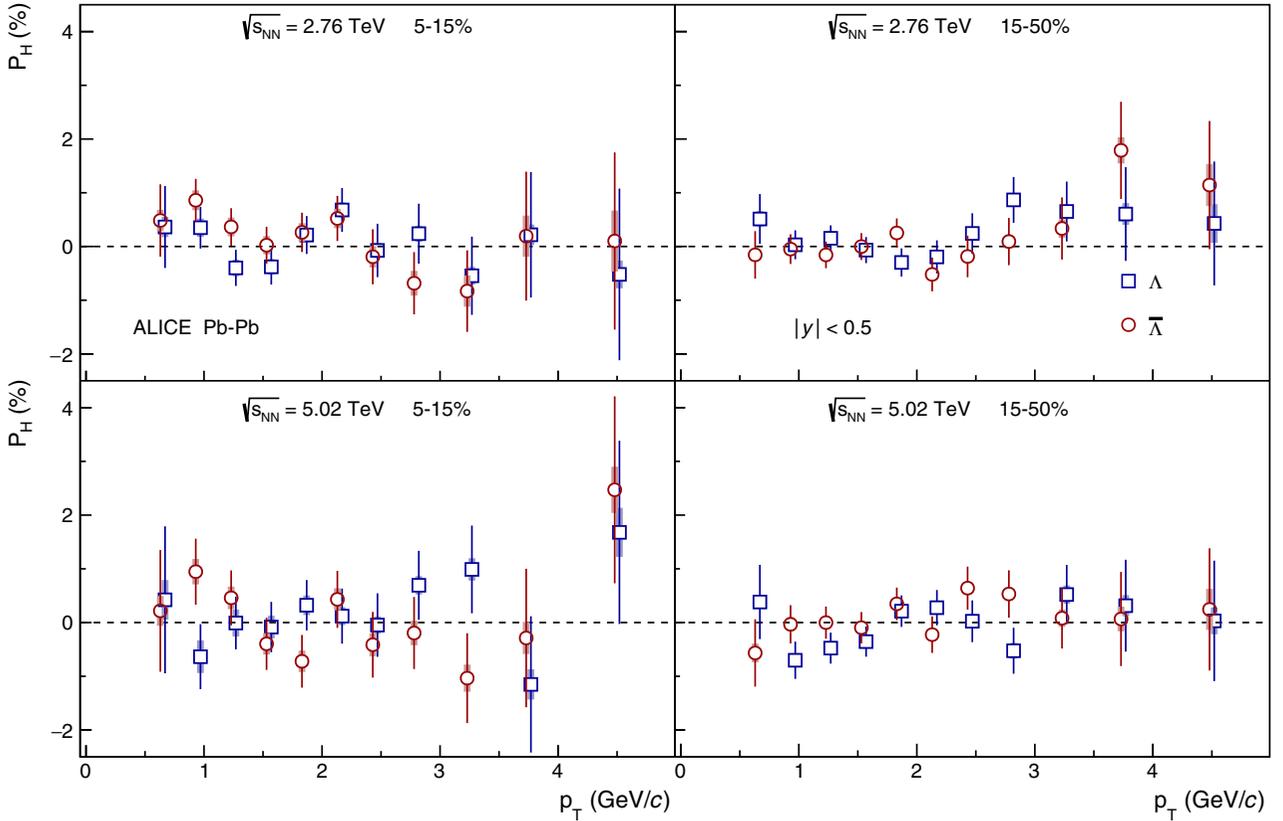

FIG. 4. The global hyperon polarization as function of transverse momentum p_T for Pb-Pb collisions at $\sqrt{s_{NN}} = 2.76$ TeV (upper) and 5.02 TeV (lower) in 5–15 (left) and 15–50 (right) centrality classes. The systematic uncertainties are shown as shaded boxes. Points are slightly shifted along the horizontal axis for better visibility.
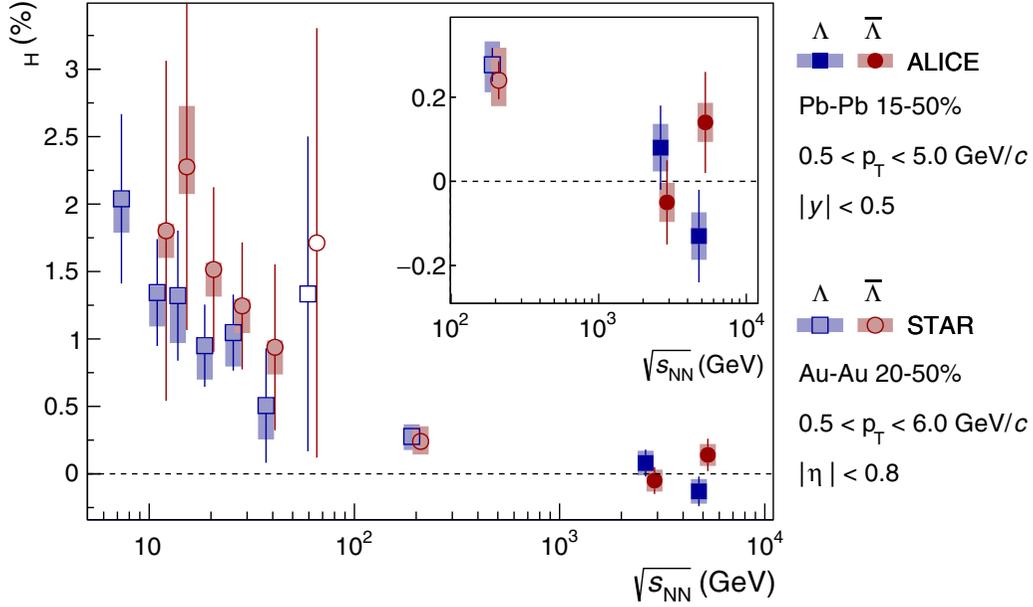
FIG. 5. The global hyperon polarization as a function of collision energy. Results are compared with the STAR data at lower energies [10,11]. The insert shows zoomed-in comparison with the data at the top RHIC energy. The systematic uncertainties are shown as shaded boxes. Points are slightly shifted along the horizontal axis for better visibility.

distribution. Using the method described in Refs. [25,42] the corresponding relative uncertainty was estimated to be about 10 independent of centrality. This uncertainty comes primarily from the admixture of the higher-order harmonics when hyperon p_T 2 GeV/c.

A detailed study was performed for the evaluation of the systematic uncertainties of $R_{\rm SP}^{(1)}$ as well as for the evaluation of the difference between the two neutron ZDC detectors. The correlations between the flow vectors from different detectors, including TPC and pairs of ZDC, V0, FMD detectors were studied. The contribution to the total systematic uncertainties due to the $R_{\rm SP}^{(1)}$ extraction were found to be at a level of a few percentages.

IV. RESULTS

Figures 3 and 4 show the measured hyperon global polarization P_H as a function of centrality and hyperon transverse momentum, p_T, in Pb-Pb collisions for two collision energies. The results from 2010 and 2011 data samples were combined accounting for the corresponding statistical and systematic uncertainty. At RHIC energies, the global polarization ex-

hibited a clear centrality dependence with three times large magnitude in peripheral collisions compared to that in central, while no significant p_T dependence within the accessible p_T range was observed [11]. The P_H at the LHC is found to be consistent with zero within the experimental uncertainties for all studied centrality classes (Fig. 3) and p_T ranges (Fig. 4). By repeating a similar analysis, no signal signal was observed as a function of rapidity either.

The average global polarization for two centrality ranges, 5–15 and 15–50, are presented in Fig. 5, while numerical values are reported in Table II. Figure 5 also presents the comparison with the STAR data [10,11] for lower collision energies. Despite large uncertainties, the ALICE measurements confirm the trend of the global polarization decreasing with increasing collision energy.

Assuming the same values of the global polarization for Λ and $\overline{\Lambda}$ and neglecting the possible difference of about 30 (according to the empirical estimates discussed above) between the two LHC energies, one can average all four ALICE data points for 15–50 centrality, where the largest signal is expected. This yields a value $\langle P_H\rangle( ) \approx 0.01 \pm 0.06$ (stat.) ± 0.03 (syst.) for 15–50 centrality, which is

TABLE II. The global polarization of Λ and $\overline{\Lambda}$ hyperons in Pb-Pb collisions at $\sqrt{s_{NN}} = 2.76$ TeV and 5.02 TeV for centrality ranges 5–15 and 15–50.

$\sqrt{s_{NN}}$	Centrality	$P_\Lambda( )$	$P_{\overline{\Lambda}}( )$
2.76 TeV	5–15	0.01 ± 0.13 (stat.) ± 0.04 (syst.)	0.09 ± 0.13 (stat.) ± 0.08 (syst.)
	15–50	0.08 ± 0.10 (stat.) ± 0.04 (syst.)	-0.05 ± 0.10 (stat.) ± 0.03 (syst.)
5.02 TeV	5–15	0.08 ± 0.18 (stat.) ± 0.08 (syst.)	-0.07 ± 0.18 (stat.) ± 0.03 (syst.)
	15–50	-0.13 ± 0.11 (stat.) ± 0.04 (syst.)	0.14 ± 0.12 (stat.) ± 0.03 (syst.)
Average	15–50	$\langle P_H\rangle( ) \approx 0.01 \pm 0.06$ (stat.) ± 0.03 (syst.)	

consistent with the empirical estimates of $P_H(\ )\approx 0.04$–0.08 based on directed flow measurements.

V. SUMMARY

The first measurements of Λ and $\overline{\Lambda}$ hyperons global polarization are reported for Pb-Pb collisions at $\sqrt{s_{NN}} = 2.76$ and 5.02 TeV recorded with ALICE at the LHC. The hyperon global polarization has been measured differentially as a function of centrality and transverse momentum (p_T) for the range of collision centrality 5–50 , $0.5 < p_T < 5$ GeV/c, and rapidity $|y| < 0.5$. No significant dependences neither splitting between the global polarization values for Λ and $\overline{\Lambda}$ has been observed. The average Λ and $\overline{\Lambda}$ polarization for 15–50 centrality range at two collision energies is found to be consistent with zero, $\langle P_H \rangle(\ ) \approx 0.01 \pm 0.06$ (stat.) $\pm$ 0.03 (syst.). This confirms the observed earlier trend of the global polarization decrease with increasing collision energy. The results are compatible with the extrapolation of the RHIC results and empirical estimates of $P_H(\ ) \approx 0.04$–0.08 based on the similarity of collision energy dependence of the global polarization and the slope of the directed flow in the midrapidity region. The high luminosity LHC run after the 2019–2021 long shutdown with the upgraded ALICE detector will bring more than 100 times more data, which should allow tests of the previously mentioned prediction with much better accuracy.

[1] Z.-T. Liang and X.-N. Wang, Globally Polarized Quark-Gluon Plasma in Non-Central A+A Collisions, Phys. Rev. Lett. **94**, 102301 (2005); **96**, 039901(E) (2006).

[2] S. A. Voloshin, Polarized secondary particles in unpolarized high energy hadron-hadron collisions? arXiv:nucl-th/0410089 [nucl-th].

[3] Z.-T. Liang and X.-N. Wang, Spin alignment of vector mesons in non-central A+A collisions, Phys. Lett. B **629**, 20 (2005).

[4] J.-H. Gao, S.-W. Chen, W.-t. Deng, Z.-T. Liang, Q. Wang, and X.-N. Wang, Global quark polarization in non-central A+A collisions, Phys. Rev. C **77**, 044902 (2008).

[5] F. Becattini, G. Inghirami, V. Rolando, A. Beraudo, L. Del Zanna, A. De Pace, M. Nardi, G. Pagliara, and V. Chandra, A study of vorticity formation in high energy nuclear collisions, Eur. Phys. J. C **75**, 406 (2015); **78**, 354(E) (2018).

[6] H. Li, L.-G. Pang, Q. Wang, and X.-L. Xia, Global Λ polarization in heavy-ion collisions from a transport model, Phys. Rev. C **96**, 054908 (2017).

[7] Y. Xie, D. Wang, and L. P. Csernai, Global Λ polarization in high-energy collisions, Phys. Rev. C **95**, 031901 (2017).

[8] V. Skokov, A. Yu. Illarionov, and V. Toneev, Estimate of the magnetic field strength in heavy-ion collisions, Int. J. Mod. Phys. A **24**, 5925 (2009).

[9] K. Tuchin, Particle production in strong electromagnetic fields in relativistic heavy-ion collisions, Adv. High Energy Phys. **2013**, 490495 (2013).

[10] L. Adamczyk *et al.* (STAR Collaboration), Global Λ hyperon polarization in nuclear collisions: evidence for the most vortical fluid, Nature **548**, 62 (2017).

[11] J. Adam *et al.* (STAR Collaboration), Global polarization of Λ hyperons in Au+Au collisions at $\sqrt{s_{NN}} = 200$ GeV, Phys. Rev. C **98**, 014910 (2018).

[12] F. Becattini, I. Karpenko, M. Lisa, I. Upsal, and S. Voloshin, Global hyperon polarization at local thermodynamic equilibrium with vorticity, magnetic field and feed-down, Phys. Rev. C **95**, 054902 (2017).

[13] I. Karpenko and F. Becattini, Study of Λ polarization in relativistic nuclear collisions at $\sqrt{s_{NN}} = 7.7$–200 GeV, Eur. Phys. J. C **77**, 213 (2017).

[14] W. Florkowski, B. Friman, A. Jaiswal, and E. Speranza, Relativistic fluid dynamics with spin, Phys. Rev. C **97**, 041901 (2018).

[15] M. Baznat, K. Gudima, A. Sorin, and O. Teryaev, Hyperon polarization in heavy-ion collisions and holographic gravitational anomaly, Phys. Rev. C **97**, 041902 (2018).

[16] S. A. Voloshin, Vorticity and particle polarization in heavy ion collisions (experimental perspective), EPJ Web Conf. **171**, 07002 (2018).

[17] F. Becattini and I. Karpenko, Collective Longitudinal Polarization in Relativistic Heavy-Ion Collisions at Very High Energy, Phys. Rev. Lett. **120**, 012302 (2018).

[18] L. Adamczyk *et al.* (STAR Collaboration), Beam-Energy Dependence of the Directed Flow of Protons, Antiprotons, and Pions in Au+Au Collisions, Phys. Rev. Lett. **112**, 162301 (2014).

[19] P. Shanmuganathan (STAR Collaboration), Beam-energy and centrality dependence of directed flow of identified particles, Nucl. Phys. A **956**, 260 (2016).

[20] B. Abelev *et al.* (ALICE Collaboration), Directed Flow of Charged Particles at Midrapidity Relative to the Spectator Plane in Pb-Pb Collisions at $\sqrt{s_{NN}}$=2.76 TeV, Phys. Rev. Lett. **111**, 232302 (2013).

[21] S. Acharya (ALICE Collaboration), Probing the effects of strong electromagnetic fields with charge-dependent directed flow in Pb-Pb collisions at the LHC, arXiv:1910.14406 [nucl-ex].

[22] L. Adamczyk *et al.* (STAR Collaboration), Azimuthal anisotropy in Cu+Au collisions at $\sqrt{s_{NN}} = 200$ GeV, Phys. Rev. C **98**, 014915 (2018).

[23] M. Tanabashi *et al.* (Particle Data Group Collaboration), Review of particle physics, Phys. Rev. D **98**, 030001 (2018).

[24] M. Ablikim *et al.* (BESIII Collaboration), Polarization and entanglement in baryon-antibaryon pair production in electron-positron annihilation, Nat. Phys. **15**, 631 (2019).

[25] B. I. Abelev *et al.* (STAR Collaboration), Global polarization measurement in Au+Au collisions, Phys. Rev. C **76**, 024915 (2007); **95**, 039906(E) (2017).

[26] S. Wheaton and J. Cleymans, THERMUS: A Thermal model package for ROOT, Comput. Phys. Commun. **180**, 84 (2009).

[27] K. Aamodt *et al.* (ALICE Collaboration), The ALICE experiment at the CERN LHC, JINST **3**, S08002 (2008).

[28] B. B. Abelev *et al.* (ALICE Collaboration), Performance of the ALICE Experiment at the CERN LHC, Int. J. Mod. Phys. A **29**, 1430044 (2014).

[29] G. Dellacasa *et al.* (ALICE Collaboration), ALICE: Technical design report of the time projection chamber, CERN-OPEN-2000-183 and CERN-LHCC-2000-001 (2000).

[30] G. Dellacasa *et al.* (ALICE Collaboration), ALICE technical design report of the inner tracking system (ITS), CERN-LHCC-99-12 (1999).

[31] G. Dellacasa *et al.* (ALICE Collaboration), ALICE technical design report of the zero degree calorimeter (ZDC), CERN-LHCC-99-05 (1999).

[32] E. Abbas *et al.* (ALICE Collaboration), Performance of the ALICE VZERO system, J. Inst. **8**, P10016 (2013).

[33] K. Aamodt *et al.* (ALICE Collaboration), Charged-Particle Multiplicity Density at Mid-Rapidity in Central Pb-Pb Collisions at $\sqrt{s_{NN}} = 2.76$ TeV, Phys. Rev. Lett. **105**, 252301 (2010).

[34] K. Aamodt *et al.* (ALICE Collaboration), Centrality Dependence of the Charged-Particle Multiplicity Density at Mid-Rapidity in Pb-Pb Collisions at $\sqrt{s_{NN}} = 2.76$ TeV, Phys. Rev. Lett. **106**, 032301 (2011).

[35] B. Abelev *et al.* (ALICE Collaboration), Centrality determination of Pb-Pb collisions at $\sqrt{s_{NN}} = 2.76$ TeV with ALICE, Phys. Rev. C **88**, 044909 (2013).

[36] I. Selyuzhenkov and S. Voloshin, Effects of non-uniform acceptance in anisotropic flow measurement, Phys. Rev. C **77**, 034904 (2008).

[37] A. M. Poskanzer and S. A. Voloshin, Methods for analyzing anisotropic flow in relativistic nuclear collisions, Phys. Rev. C **58**, 1671 (1998).

[38] D. Macina and N. De Marco, Modification IR2 to solve the ALICE ZDC-TCTVB interference problem, LHC-LJ-EC-0025 (2011).

[39] P. Cortese *et al.* (ALICE Collaboration), ALICE technical design report on forward detectors: FMD, T0 and V0, CERN-LHCC-2004-025 (2004).

[40] S. Acharya *et al.* (ALICE Collaboration), Anisotropic flow of identified particles in Pb-Pb collisions at $\sqrt{s_{NN}} = 5.02$ TeV, J. High Energy Phys. 09 (2018) 006.

[41] R. Barlow, Systematic errors: Facts and fictions, arXiv:hep-ex/0207026 [hep-ex].

[42] I. Selyuzhenkov (STAR Collaboration), Acceptance effects in the hyperons global polarization measurement, AIP Conf. Proc. **870**, 712 (2006).

S. Acharya,[141] D. Adamová,[93] S. P. Adhya,[141] A. Adler,[73] J. Adolfsson,[79] M. M. Aggarwal,[98] G. Aglieri Rinella,[34] M. Agnello,[31] N. Agrawal,[10,48,53] Z. Ahammed,[141] S. Ahmad,[17] S. U. Ahn,[75] A. Akindinov,[90] M. Al-Turany,[105] S. N. Alam,[141] D. S. D. Albuquerque,[122] D. Aleksandrov,[86] B. Alessandro,[58] H. M. Alfanda,[6] R. Alfaro Molina,[71] B. Ali,[17] Y. Ali,[15] A. Alici,[10,27,53] A. Alkin,[2] J. Alme,[22] T. Alt,[68] L. Altenkamper,[22] I. Altsybeev,[112] M. N. Anaam,[6] C. Andrei,[47] D. Andreou,[34] H. A. Andrews,[109] A. Andronic,[144] M. Angeletti,[34] V. Anguelov,[102] C. Anson,[16] T. Antičić,[106] F. Antinori,[56] P. Antonioli,[53] R. Anwar,[125] N. Apadula,[78] L. Aphecetche,[114] H. Appelshäuser,[68] S. Arcelli,[27] R. Arnaldi,[58] M. Arratia,[78] I. C. Arsene,[21] M. Arslandok,[102] A. Augustinus,[34] R. Averbeck,[105] S. Aziz,[61] M. D. Azmi,[17] A. Badalà,[55] Y. W. Baek,[40] S. Bagnasco,[58] X. Bai,[105] R. Bailhache,[68] R. Bala,[99] A. Baldisseri,[137] M. Ball,[42] S. Balouza,[103] R. C. Baral,[84] R. Barbera,[28] L. Barioglio,[26] G. G. Barnaföldi,[145] L. S. Barnby,[92] V. Barret,[134] P. Bartalini,[6] K. Barth,[34] E. Bartsch,[68] F. Baruffaldi,[29] N. Bastid,[134] S. Basu,[143] G. Batigne,[114] B. Batyunya,[74] P. C. Batzing,[21] D. Bauri,[48] J. L. Bazo Alba,[110] I. G. Bearden,[87] C. Bedda,[63] N. K. Behera,[60] I. Belikov,[136] F. Bellini,[34] R. Bellwied,[125] V. Belyaev,[91] G. Bencedi,[145] S. Beole,[26] A. Bercuci,[47] Y. Berdnikov,[96] D. Berenyi,[145] R. A. Bertens,[130] D. Berzano,[58] M. G. Besoiu,[67] L. Betev,[34] A. Bhasin,[99] I. R. Bhat,[99] M. A. Bhat,[3] H. Bhatt,[48] B. Bhattacharjee,[41] A. Bianchi,[26] L. Bianchi,[26] N. Bianchi,[51] J. Bielčík,[37] J. Bielčíková,[93] A. Bilandzic,[103,117] G. Biro,[145] R. Biswas,[3] S. Biswas,[3] J. T. Blair,[119] D. Blau,[86] C. Blume,[68] G. Boca,[139] F. Bock,[34,94] A. Bogdanov,[91] L. Boldizsár,[145] A. Bolozdynya,[91] M. Bombara,[38] G. Bonomi,[140] H. Borel,[137] A. Borissov,[91,144] M. Borri,[127] H. Bossi,[146] E. Botta,[26] L. Bratrud,[68] P. Braun-Munzinger,[105] M. Bregant,[121] T. A. Broker,[68] M. Broz,[37] E. J. Brucken,[43] E. Bruna,[58] G. E. Bruno,[33,104] M. D. Buckland,[127] D. Budnikov,[107] H. Buesching,[68] S. Bufalino,[31] O. Bugnon,[114] P. Buhler,[113] P. Buncic,[34] Z. Buthelezi,[72] J. B. Butt,[15] J. T. Buxton,[95] S. A. Bysiak,[118] D. Caffarri,[88] A. Caliva,[105] E. Calvo Villar,[110] R. S. Camacho,[44] P. Camerini,[25] A. A. Capon,[113] F. Carnesecchi,[10,27] J. Castillo Castellanos,[137] A. J. Castro,[130] E. A. R. Casula,[54] F. Catalano,[31] C. Ceballos Sanchez,[52] P. Chakraborty,[48] S. Chandra,[141] B. Chang,[126] W. Chang,[6] S. Chapeland,[34] M. Chartier,[127] S. Chattopadhyay,[141] S. Chattopadhyay,[108] A. Chauvin,[24] C. Cheshkov,[135] B. Cheynis,[135] V. Chibante Barroso,[34] D. D. Chinellato,[122] S. Cho,[60] P. Chochula,[34] T. Chowdhury,[134] P. Christakoglou,[88] C. H. Christensen,[87] P. Christiansen,[79] T. Chujo,[133] C. Cicalo,[54] L. Cifarelli,[10,27] F. Cindolo,[53] J. Cleymans,[124] F. Colamaria,[52] D. Colella,[52] A. Collu,[78] M. Colocci,[27] M. Concas,[58,a] G. Conesa Balbastre,[77] Z. Conesa del Valle,[61] G. Contin,[59,127] J. G. Contreras,[37] T. M. Cormier,[94] Y. Corrales Morales,[26,58] P. Cortese,[32] M. R. Cosentino,[123] F. Costa,[34] S. Costanza,[139] P. Crochet,[134] E. Cuautle,[69] P. Cui,[6] L. Cunqueiro,[94] D. Dabrowski,[142] T. Dahms,[103,117] A. Dainese,[56] F. P. A. Damas,[114,137] S. Dani,[65] M. C. Danisch,[102] A. Danu,[67] D. Das,[108] I. Das,[108] P. Das,[3] S. Das,[3] A. Dash,[84] S. Dash,[48] A. Dashi,[103] S. De,[49,84] A. De Caro,[30] G. de Cataldo,[52] C. de Conti,[121] J. de Cuveland,[39] A. De Falco,[24] D. De Gruttola,[10] N. De Marco,[58] S. De Pasquale,[30] R. D. De Souza,[122] S. Deb,[49] H. F. Degenhardt,[121] K. R. Deja,[142] A. Deloff,[83] S. Delsanto,[26,131] D. Devetak,[105] P. Dhankher,[48] D. Di Bari,[33] A. Di Mauro,[34] R. A. Diaz,[8] T. Dietel,[124] P. Dillenseger,[68] Y. Ding,[6] R. Divià,[34] Ø. Djuvsland,[22] U. Dmitrieva,[62] A. Dobrin,[34,67] B. Dönigus,[68] O. Dordic,[21] A. K. Dubey,[141] A. Dubla,[105] S. Dudi,[98] M. Dukhishyam,[84] P. Dupieux,[134] R. J. Ehlers,[146] D. Elia,[52] H. Engel,[73] E. Epple,[146] B. Erazmus,[114] F. Erhardt,[97] A. Erokhin,[112] M. R. Ersdal,[22] B. Espagnon,[61] G. Eulisse,[34] J. Eum,[18] D. Evans,[109] S. Evdokimov,[89] L. Fabbietti,[103,117] M. Faggin,[29] J. Faivre,[77] F. Fan,[6] A. Fantoni,[51] M. Fasel,[94] P. Fecchio,[31] A. Feliciello,[58] G. Feofilov,[112] A. Fernández Téllez,[44] A. Ferrero,[137] A. Ferretti,[26] A. Festanti,[34] V. J. G. Feuillard,[102] J. Figiel,[118] S. Filchagin,[107] D. Finogeev,[62] F. M. Fionda,[22] G. Fiorenza,[52] F. Flor,[125] S. Foertsch,[72] P. Foka,[105] S. Fokin,[86] E. Fragiacomo,[59] U. Frankenfeld,[105] G. G. Fronze,[26] U. Fuchs,[34] C. Furget,[77] A. Furs,[62] M. Fusco Girard,[30] J. J. Gaardhøje,[87] M. Gagliardi,[26] A. M. Gago,[110] A. Gal,[136] C. D. Galvan,[120] P. Ganoti,[82] C. Garabatos,[105] E. Garcia-Solis,[11] K. Garg,[28] C. Gargiulo,[34] A. Garibli,[85] K. Garner,[144] P. Gasik,[103,117] E. F. Gauger,[119] M. B. Gay Ducati,[70] M. Germain,[114] J. Ghosh,[108] P. Ghosh,[141] S. K. Ghosh,[3] P. Gianotti,[51] P. Giubellino,[58,105] P. Giubilato,[29] P. Glässel,[102] D. M. Gómez Coral,[71] A. Gomez Ramirez,[73] V. Gonzalez,[105] P. González-Zamora,[44] S. Gorbunov,[39] L. Görlich,[118] S. Gotovac,[35] V. Grabski,[71] L. K. Graczykowski,[142] K. L. Graham,[109] L. Greiner,[78] A. Grelli,[63] C. Grigoras,[34] V. Grigoriev,[91] A. Grigoryan,[1] S. Grigoryan,[74] O. S. Groettvik,[22] F. Grosa,[31] J. F. Grosse-Oetringhaus,[34] R. Grosso,[105] R. Guernane,[77] B. Guerzoni,[27] M. Guittiere,[114] K. Gulbrandsen,[87] T. Gunji,[132] A. Gupta,[99] R. Gupta,[99] I. B. Guzman,[44] R. Haake,[146] M. K. Habib,[105] C. Hadjidakis,[61] H. Hamagaki,[80] G. Hamar,[145] M. Hamid,[6] R. Hannigan,[119] M. R. Haque,[63] A. Harlenderova,[105] J. W. Harris,[146] A. Harton,[11] J. A. Hasenbichler,[34] H. Hassan,[77] D. Hatzifotiadou,[10,53] P. Hauer,[42] S. Hayashi,[132] A. D. L. B. Hechavarria,[144] S. T. Heckel,[68] E. Hellbär,[68] H. Helstrup,[36] A. Herghelegiu,[47] E. G. Hernandez,[44] G. Herrera Corral,[9] F. Herrmann,[144] K. F. Hetland,[36] T. E. Hilden,[43] H. Hillemanns,[34] C. Hills,[127] B. Hippolyte,[136] B. Hohlweger,[103] D. Horak,[37] S. Hornung,[105] R. Hosokawa,[16,133] P. Hristov,[34] C. Huang,[61] C. Hughes,[130] P. Huhn,[68]

T. J. Humanic,[95] H. Hushnud,[108] L. A. Husova,[144] N. Hussain,[41] S. A. Hussain,[15] D. Hutter,[39] D. S. Hwang,[19] J. P. Iddon,[34,127] R. Ilkaev,[107] M. Inaba,[133] M. Ippolitov,[86] M. S. Islam,[108] M. Ivanov,[105] V. Ivanov,[96] V. Izucheev,[89] B. Jacak,[78] N. Jacazio,[27,53] P. M. Jacobs,[78] M. B. Jadhav,[48] S. Jadlovska,[116] J. Jadlovsky,[116] S. Jaelani,[63] C. Jahnke,[121] M. J. Jakubowska,[142] M. A. Janik,[142] M. Jercic,[97] O. Jevons,[109] R. T. Jimenez Bustamante,[105] M. Jin,[125] F. Jonas,[94,144] P. G. Jones,[109] A. Jusko,[109] P. Kalinak,[64] A. Kalweit,[34] J. H. Kang,[147] V. Kaplin,[91] S. Kar,[6] A. Karasu Uysal,[76] O. Karavichev,[62] T. Karavicheva,[62] P. Karczmarczyk,[34] E. Karpechev,[62] U. Kebschull,[73] R. Keidel,[46] M. Keil,[34] B. Ketzer,[42] Z. Khabanova,[88] A. M. Khan,[6] S. Khan,[17] S. A. Khan,[141] A. Khanzadeev,[96] Y. Kharlov,[89] A. Khatun,[17] A. Khuntia,[49,118] B. Kileng,[36] B. Kim,[60] B. Kim,[133] D. Kim,[147] D. J. Kim,[126] E. J. Kim,[13] H. Kim,[147] J. Kim,[147] J. S. Kim,[40] J. Kim,[102] J. Kim,[147] J. Kim,[13] M. Kim,[102] S. Kim,[19] T. Kim,[147] T. Kim,[147] S. Kirsch,[39] I. Kisel,[39] S. Kiselev,[90] A. Kisiel,[142] J. L. Klay,[5] C. Klein,[68] J. Klein,[58] S. Klein,[78] C. Klein-Bösing,[144] S. Klewin,[102] A. Kluge,[34] M. L. Knichel,[34] A. G. Knospe,[125] C. Kobdaj,[115] M. K. Köhler,[102] T. Kollegger,[105] A. Kondratyev,[74] N. Kondratyeva,[91] E. Kondratyuk,[89] P. J. Konopka,[34] M. Konyushikhin,[143] L. Koska,[116] O. Kovalenko,[83] V. Kovalenko,[112] M. Kowalski,[118] I. Králik,[64] A. Kravčáková,[38] L. Kreis,[105] M. Krivda,[64,109] F. Krizek,[93] K. Krizkova Gajdosova,[37] M. Krüger,[68] E. Kryshen,[96] M. Krzewicki,[39] A. M. Kubera,[95] V. Kučera,[60] C. Kuhn,[136] P. G. Kuijer,[88] L. Kumar,[98] S. Kumar,[48] S. Kundu,[84] P. Kurashvili,[83] A. Kurepin,[62] A. B. Kurepin,[62] A. Kuryakin,[107] S. Kushpil,[93] J. Kvapil,[109] M. J. Kweon,[60] J. Y. Kwon,[60] Y. Kwon,[147] S. L. La Pointe,[39] P. La Rocca,[28] Y. S. Lai,[78] R. Langoy,[129] K. Lapidus,[34,146] A. Lardeux,[21] P. Larionov,[51] E. Laudi,[34] R. Lavicka,[37] T. Lazareva,[112] R. Lea,[25] L. Leardini,[102] S. Lee,[147] F. Lehas,[88] S. Lehner,[113] J. Lehrbach,[39] R. C. Lemmon,[92] I. León Monzón,[120] E. D. Lesser,[20] M. Lettrich,[34] P. Lévai,[145] X. Li,[12] X. L. Li,[6] J. Lien,[129] R. Lietava,[109] B. Lim,[18] S. Lindal,[21] V. Lindenstruth,[39] S. W. Lindsay,[127] C. Lippmann,[105] M. A. Lisa,[95] V. Litichevskyi,[43] A. Liu,[78] S. Liu,[95] W. J. Llope,[143] I. M. Lofnes,[22] V. Loginov,[91] C. Loizides,[94] P. Loncar,[35] X. Lopez,[134] E. López Torres,[8] P. Luettig,[68] J. R. Luhder,[144] M. Lunardon,[29] G. Luparello,[59] A. Maevskaya,[62] M. Mager,[34] S. M. Mahmood,[21] T. Mahmoud,[42] A. Maire,[136] R. D. Majka,[146] M. Malaev,[96] Q. W. Malik,[21] L. Malinina,[74,b] D. Mal'Kevich,[90] P. Malzacher,[105] G. Mandaglio,[55] V. Manko,[86] F. Manso,[134] V. Manzari,[52] Y. Mao,[6] M. Marchisone,[135] J. Mareš,[66] G. V. Margagliotti,[25] A. Margotti,[53] J. Margutti,[63] A. Marín,[105] C. Markert,[119] M. Marquard,[68] N. A. Martin,[102] P. Martinengo,[34] J. L. Martinez,[125] M. I. Martínez,[44] G. Martínez García,[114] M. Martinez Pedreira,[34] S. Masciocchi,[105] M. Masera,[26] A. Masoni,[54] L. Massacrier,[61] E. Masson,[114] A. Mastroserio,[52,138] A. M. Mathis,[103,117] O. Matonoha,[79] P. F. T. Matuoka,[121] A. Matyja,[118] C. Mayer,[118] M. Mazzilli,[33] M. A. Mazzoni,[57] A. F. Mechler,[68] F. Meddi,[23] Y. Melikyan,[62,91] A. Menchaca-Rocha,[71] C. Mengke,[6] E. Meninno,[30] M. Meres,[14] S. Mhlanga,[124] Y. Miake,[133] L. Micheletti,[26] M. M. Mieskolainen,[43] D. L. Mihaylov,[103] K. Mikhaylov,[74,90] A. Mischke,[63,c] A. N. Mishra,[69] D. Miśkowiec,[105] C. M. Mitu,[67] A. Modak,[3] N. Mohammadi,[34] A. P. Mohanty,[63] B. Mohanty,[84] M. Mohisin Khan,[17,d] M. Mondal,[141] C. Mordasini,[103] D. A. Moreira De Godoy,[144] L. A. P. Moreno,[44] S. Moretto,[29] A. Morreale,[114] A. Morsch,[34] T. Mrnjavac,[34] V. Muccifora,[51] E. Mudnic,[35] D. Mühlheim,[144] S. Muhuri,[141] J. D. Mulligan,[78] M. G. Munhoz,[121] K. Münning,[42] R. H. Munzer,[68] H. Murakami,[132] S. Murray,[124] L. Musa,[34] J. Musinsky,[64] C. J. Myers,[125] J. W. Myrcha,[142] B. Naik,[48] R. Nair,[83] B. K. Nandi,[48] R. Nania,[10,53] E. Nappi,[52] M. U. Naru,[15] A. F. Nassirpour,[79] H. Natal da Luz,[121] C. Nattrass,[130] R. Nayak,[48] T. K. Nayak,[84,141] S. Nazarenko,[107] A. Neagu,[21] R. A. Negrao De Oliveira,[68] L. Nellen,[69] S. V. Nesbo,[36] G. Neskovic,[39] D. Nesterov,[112] B. S. Nielsen,[87] S. Nikolaev,[86] S. Nikulin,[86] V. Nikulin,[96] F. Noferini,[10,53] P. Nomokonov,[74] G. Nooren,[63] J. Norman,[77] N. Novitzky,[133] P. Nowakowski,[142] A. Nyanin,[86] J. Nystrand,[22] M. Ogino,[80] A. Ohlson,[102] J. Oleniacz,[142] A. C. Oliveira Da Silva,[121] M. H. Oliver,[146] C. Oppedisano,[58] R. Orava,[43] A. Ortiz Velasquez,[69] A. Oskarsson,[79] J. Otwinowski,[118] K. Oyama,[80] Y. Pachmayer,[102] V. Pacik,[87] D. Pagano,[140] G. Paić,[69] P. Palni,[6] J. Pan,[143] A. K. Pandey,[48] S. Panebianco,[137] P. Pareek,[49] J. Park,[60] J. E. Parkkila,[126] S. Parmar,[98] S. P. Pathak,[125] R. N. Patra,[141] B. Paul,[24,58] H. Pei,[6] T. Peitzmann,[63] X. Peng,[6] L. G. Pereira,[70] H. Pereira Da Costa,[137] D. Peresunko,[86] G. M. Perez,[8] E. Perez Lezama,[68] V. Peskov,[68] Y. Pestov,[4] V. Petráček,[37] M. Petrovici,[47] R. P. Pezzi,[70] S. Piano,[59] M. Pikna,[14] P. Pillot,[114] L. O. D. L. Pimentel,[87] O. Pinazza,[34,53] L. Pinsky,[125] C. Pinto,[28] S. Pisano,[51] D. Pistone,[55] D. B. Piyarathna,[125] M. Płoskoń,[78] M. Planinic,[97] F. Pliquett,[68] J. Pluta,[142] S. Pochybova,[145] M. G. Poghosyan,[94] B. Polichtchouk,[89] N. Poljak,[97] A. Pop,[47] H. Poppenborg,[144] S. Porteboeuf-Houssais,[134] V. Pozdniakov,[74] S. K. Prasad,[3] R. Preghenella,[53] F. Prino,[58] C. A. Pruneau,[143] I. Pshenichnov,[62] M. Puccio,[26,34] V. Punin,[107] K. Puranapanda,[141] J. Putschke,[143] R. E. Quishpe,[125] S. Ragoni,[109] S. Raha,[3] S. Rajput,[99] J. Rak,[126] A. Rakotozafindrabe,[137] L. Ramello,[32] F. Rami,[136] R. Raniwala,[100] S. Raniwala,[100] S. S. Räsänen,[43] B. T. Rascanu,[68] R. Rath,[49] V. Ratza,[42] I. Ravasenga,[31] K. F. Read,[94,130] K. Redlich,[83,e] A. Rehman,[22] P. Reichelt,[68] F. Reidt,[34] X. Ren,[6] R. Renfordt,[68] A. Reshetin,[62] J.-P. Revol,[10] K. Reygers,[102] V. Riabov,[96] T. Richert,[79,87] M. Richter,[21] P. Riedler,[34] W. Riegler,[34] F. Riggi,[28] C. Ristea,[67] S. P. Rode,[49] M. Rodríguez Cahuantzi,[44] K. Røed,[21] R. Rogalev,[89] E. Rogochaya,[74] D. Rohr,[34] D. Röhrich,[22] P. S. Rokita,[142] F. Ronchetti,[51] E. D. Rosas,[69] K. Roslon,[142] P. Rosnet,[134] A. Rossi,[29,56] A. Rotondi,[139] F. Roukoutakis,[82] A. Roy,[49] P. Roy,[108] O. V. Rueda,[79] R. Rui,[25] B. Rumyantsev,[74] A. Rustamov,[85] E. Ryabinkin,[86] Y. Ryabov,[96] A. Rybicki,[118] H. Rytkonen,[126] S. Sadhu,[141] S. Sadovsky,[89] K. Šafařík,[34,37] S. K. Saha,[141] B. Sahoo,[48] P. Sahoo,[48,49] R. Sahoo,[49] S. Sahoo,[65] P. K. Sahu,[65] J. Saini,[141] S. Sakai,[133] S. Sambyal,[99] V. Samsonov,[91,96] F. R. Sanchez,[44] A. Sandoval,[71] A. Sarkar,[72] D. Sarkar,[143] N. Sarkar,[141] P. Sarma,[41] V. M. Sarti,[103] M. H. P. Sas,[63] E. Scapparone,[53] B. Schaefer,[94] J. Schambach,[119] H. S. Scheid,[68] C. Schiaua,[47] R. Schicker,[102] A. Schmah,[102] C. Schmidt,[105] H. R. Schmidt,[101] M. O. Schmidt,[102] M. Schmidt,[101] N. V. Schmidt,[68,94] A. R. Schmier,[130] J. Schukraft,[34,87] Y. Schutz,[34,136] K. Schwarz,[105] K. Schweda,[105] G. Scioli,[27] E. Scomparin,[58] M. Šefčík,[38] J. E. Seger,[16] Y. Sekiguchi,[132] D. Sekihata,[45,132] I. Selyuzhenkov,[91,105] S. Senyukov,[136] D. Serebryakov,[62] E. Serradilla,[71] P. Sett,[48] A. Sevcenco,[67] A. Shabanov,[62] A. Shabetai,[114] R. Shahoyan,[34] W. Shaikh,[108]

A. Shangaraev,[89] A. Sharma,[98] A. Sharma,[99] H. Sharma,[118] M. Sharma,[99] N. Sharma,[98] A. I. Sheikh,[141] K. Shigaki,[45] M. Shimomura,[81] S. Shirinkin,[90] Q. Shou,[111] Y. Sibiriak,[86] S. Siddhanta,[54] T. Siemiarczuk,[83] D. Silvermyr,[79] C. Silvestre,[77] G. Simatovic,[88] G. Simonetti,[34,103] R. Singh,[84] R. Singh,[99] V. K. Singh,[141] V. Singhal,[141] T. Sinha,[108] B. Sitar,[14] M. Sitta,[32] T. B. Skaali,[21] M. Slupecki,[126] N. Smirnov,[146] R. J. M. Snellings,[63] T. W. Snellman,[43,126] J. Sochan,[116] C. Soncco,[110] J. Song,[60,125] A. Songmoolnak,[115] F. Soramel,[29] S. Sorensen,[130] I. Sputowska,[118] J. Stachel,[102] I. Stan,[67] P. Stankus,[94] P. J. Steffanic,[130] E. Stenlund,[79] D. Stocco,[114] M. M. Storetvedt,[36] P. Strmen,[14] A. A. P. Suaide,[121] T. Sugitate,[45] C. Suire,[61] M. Suleymanov,[15] M. Suljic,[34] R. Sultanov,[90] M. Šumbera,[93] S. Sumowidagdo,[50] K. Suzuki,[113] S. Swain,[65] A. Szabo,[14] I. Szarka,[14] U. Tabassam,[15] G. Taillepied,[134] J. Takahashi,[122] G. J. Tambave,[22] S. Tang,[6,134] M. Tarhini,[114] M. G. Tarzila,[47] A. Tauro,[34] G. Tejeda Muñoz,[44] A. Telesca,[34] C. Terrevoli,[29,125] D. Thakur,[49] S. Thakur,[141] D. Thomas,[119] F. Thoresen,[87] R. Tieulent,[135] A. Tikhonov,[62] A. R. Timmins,[125] A. Toia,[68] N. Topilskaya,[62] M. Toppi,[51] F. Torales-Acosta,[20] S. R. Torres,[120] A. Trifiro,[55] S. Tripathy,[49] T. Tripathy,[48] S. Trogolo,[29] G. Trombetta,[33] L. Tropp,[38] V. Trubnikov,[2] W. H. Trzaska,[126] T. P. Trzcinski,[142] B. A. Trzeciak,[63] T. Tsuji,[132] A. Tumkin,[107] R. Turrisi,[56] T. S. Tveter,[21] K. Ullaland,[22] E. N. Umaka,[125] A. Uras,[135] G. L. Usai,[24] A. Utrobicic,[97] M. Vala,[38,116] N. Valle,[139] S. Vallero,[58] N. van der Kolk,[63] L. V. R. van Doremalen,[63] M. van Leeuwen,[63] P. Vande Vyvre,[34] D. Varga,[145] Z. Varga,[145] M. Varga-Kofarago,[145] A. Vargas,[44] M. Vargyas,[126] R. Varma,[48] M. Vasileiou,[82] A. Vasiliev,[86] O. Vázquez Doce,[103,117] V. Vechernin,[112] A. M. Veen,[63] E. Vercellin,[26] S. Vergara Limón,[44] L. Vermunt,[63] R. Vernet,[7] R. Vértesi,[145] M. G. D. L. C. Vicencio,[9] L. Vickovic,[35] J. Viinikainen,[126] Z. Vilakazi,[131] O. Villalobos Baillie,[109] A. Villatoro Tello,[44] G. Vino,[52] A. Vinogradov,[86] T. Virgili,[30] V. Vislavicius,[87] A. Vodopyanov,[74] B. Volkel,[34] M. A. Völkl,[101] K. Voloshin,[90] S. A. Voloshin,[143] G. Volpe,[33] B. von Haller,[34] I. Vorobyev,[103] D. Voscek,[116] J. Vrláková,[38] B. Wagner,[22] M. Weber,[113] S. G. Weber,[105,144] A. Wegrzynek,[34] D. F. Weiser,[102] S. C. Wenzel,[34] J. P. Wessels,[144] E. Widmann,[113] J. Wiechula,[68] J. Wikne,[21] G. Wilk,[83] J. Wilkinson,[53] G. A. Willems,[34] E. Willsher,[109] B. Windelband,[102] W. E. Witt,[130] Y. Wu,[128] R. Xu,[6] S. Yalcin,[76] K. Yamakawa,[45] S. Yang,[22] S. Yano,[137] Z. Yin,[6] H. Yokoyama,[63,133] I.-K. Yoo,[18] J. H. Yoon,[60] S. Yuan,[22] A. Yuncu,[102] V. Yurchenko,[2] V. Zaccolo,[25,58] A. Zaman,[15] C. Zampolli,[34] H. J. C. Zanoli,[63,121] N. Zardoshti,[34] A. Zarochentsev,[112] P. Závada,[66] N. Zaviyalov,[107] H. Zbroszczyk,[142] M. Zhalov,[96] X. Zhang,[6] Z. Zhang,[6] C. Zhao,[21] V. Zherebchevskii,[112] N. Zhigareva,[90] D. Zhou,[6] Y. Zhou,[87] Z. Zhou,[22] J. Zhu,[6] Y. Zhu,[6] A. Zichichi,[10,27] M. B. Zimmermann,[34] G. Zinovjev,[2] and N. Zurlo[140]

(ALICE Collaboration)

[1]*A.I. Alikhanyan National Science Laboratory (Yerevan Physics Institute) Foundation, Yerevan, Armenia*
[2]*Bogolyubov Institute for Theoretical Physics, National Academy of Sciences of Ukraine, Kiev, Ukraine*
[3]*Bose Institute, Department of Physics and Centre for Astroparticle Physics and Space Science (CAPSS), Kolkata, India*
[4]*Budker Institute for Nuclear Physics, Novosibirsk, Russia*
[5]*California Polytechnic State University, San Luis Obispo, California, USA*
[6]*Central China Normal University, Wuhan, China*
[7]*Centre de Calcul de l IN2P3, Villeurbanne, Lyon, France*
[8]*Centro de Aplicaciones Tecnológicas y Desarrollo Nuclear (CEADEN), Havana, Cuba*
[9]*Centro de Investigación y de Estudios Avanzados (CINVESTAV), Mexico City and Mérida, Mexico*
[10]*Centro Fermi–Museo Storico della Fisica e Centro Studi e Ricerche "Enrico Fermi , Rome, Italy*
[11]*Chicago State University, Chicago, Illinois, USA*
[12]*China Institute of Atomic Energy, Beijing, China*
[13]*Chonbuk National University, Jeonju, Republic of Korea*
[14]*Comenius University Bratislava, Faculty of Mathematics, Physics and Informatics, Bratislava, Slovakia*
[15]*COMSATS University Islamabad, Islamabad, Pakistan*
[16]*Creighton University, Omaha, Nebraska, USA*
[17]*Department of Physics, Aligarh Muslim University, Aligarh, India*
[18]*Department of Physics, Pusan National University, Pusan, Republic of Korea*
[19]*Department of Physics, Sejong University, Seoul, Republic of Korea*
[20]*Department of Physics, University of California, Berkeley, California, USA*
[21]*Department of Physics, University of Oslo, Oslo, Norway*
[22]*Department of Physics and Technology, University of Bergen, Bergen, Norway*
[23]*Dipartimento di Fisica dell Università La Sapienza and Sezione INFN, Rome, Italy*
[24]*Dipartimento di Fisica dell Università and Sezione INFN, Cagliari, Italy*
[25]*Dipartimento di Fisica dell Università and Sezione INFN, Trieste, Italy*
[26]*Dipartimento di Fisica dell Università and Sezione INFN, Turin, Italy*
[27]*Dipartimento di Fisica e Astronomia dell Università and Sezione INFN, Bologna, Italy*
[28]*Dipartimento di Fisica e Astronomia dell Università and Sezione INFN, Catania, Italy*
[29]*Dipartimento di Fisica e Astronomia dell Università and Sezione INFN, Padova, Italy*
[30]*Dipartimento di Fisica 'E.R. Caianiello dell Università and Gruppo Collegato INFN, Salerno, Italy*

[31]*Dipartimento DISAT del Politecnico and Sezione INFN, Turin, Italy*

[32]*Dipartimento di Scienze e Innovazione Tecnologica dell Università del Piemonte Orientale and INFN Sezione di Torino, Alessandria, Italy*

[33]*Dipartimento Interateneo di Fisica 'M. Merlin and Sezione INFN, Bari, Italy*

[34]*European Organization for Nuclear Research (CERN), Geneva, Switzerland*

[35]*Faculty of Electrical Engineering, Mechanical Engineering and Naval Architecture, University of Split, Split, Croatia*

[36]*Faculty of Engineering and Science, Western Norway University of Applied Sciences, Bergen, Norway*

[37]*Faculty of Nuclear Sciences and Physical Engineering, Czech Technical University in Prague, Prague, Czech Republic*

[38]*Faculty of Science, P.J. Šafárik University, Košice, Slovakia*

[39]*Frankfurt Institute for Advanced Studies, Johann Wolfgang Goethe-Universität Frankfurt, Frankfurt, Germany*

[40]*Gangneung-Wonju National University, Gangneung, Republic of Korea*

[41]*Gauhati University, Department of Physics, Guwahati, India*

[42]*Helmholtz-Institut für Strahlen- und Kernphysik, Rheinische Friedrich-Wilhelms-Universität Bonn, Bonn, Germany*

[43]*Helsinki Institute of Physics (HIP), Helsinki, Finland*

[44]*High Energy Physics Group, Universidad Autónoma de Puebla, Puebla, Mexico*

[45]*Hiroshima University, Hiroshima, Japan*

[46]*Hochschule Worms, Zentrum für Technologietransfer und Telekommunikation (ZTT), Worms, Germany*

[47]*Horia Hulubei National Institute of Physics and Nuclear Engineering, Bucharest, Romania*

[48]*Indian Institute of Technology Bombay (IIT), Mumbai, India*

[49]*Indian Institute of Technology Indore, Indore, India*

[50]*Indonesian Institute of Sciences, Jakarta, Indonesia*

[51]*INFN, Laboratori Nazionali di Frascati, Frascati, Italy*

[52]*INFN, Sezione di Bari, Bari, Italy*

[53]*INFN, Sezione di Bologna, Bologna, Italy*

[54]*INFN, Sezione di Cagliari, Cagliari, Italy*

[55]*INFN, Sezione di Catania, Catania, Italy*

[56]*INFN, Sezione di Padova, Padova, Italy*

[57]*INFN, Sezione di Roma, Rome, Italy*

[58]*INFN, Sezione di Torino, Turin, Italy*

[59]*INFN, Sezione di Trieste, Trieste, Italy*

[60]*Inha University, Incheon, Republic of Korea*

[61]*Institut de Physique Nucléaire d Orsay (IPNO), Institut National de Physique Nucléaire et de Physique des Particules (IN2P3/CNRS), Université de Paris-Sud, Université Paris-Saclay, Orsay, France*

[62]*Institute for Nuclear Research, Academy of Sciences, Moscow, Russia*

[63]*Institute for Subatomic Physics, Utrecht University/Nikhef, Utrecht, Netherlands*

[64]*Institute of Experimental Physics, Slovak Academy of Sciences, Košice, Slovakia*

[65]*Institute of Physics, Homi Bhabha National Institute, Bhubaneswar, India*

[66]*Institute of Physics of the Czech Academy of Sciences, Prague, Czech Republic*

[67]*Institute of Space Science (ISS), Bucharest, Romania*

[68]*Institut für Kernphysik, Johann Wolfgang Goethe-Universität Frankfurt, Frankfurt, Germany*

[69]*Instituto de Ciencias Nucleares, Universidad Nacional Autónoma de México, Mexico City, Mexico*

[70]*Instituto de Física, Universidade Federal do Rio Grande do Sul (UFRGS), Porto Alegre, Brazil*

[71]*Instituto de Física, Universidad Nacional Autónoma de México, Mexico City, Mexico*

[72]*iThemba LABS, National Research Foundation, Somerset West, South Africa*

[73]*Johann-Wolfgang-Goethe Universität Frankfurt Institut für Informatik, Fachbereich Informatik und Mathematik, Frankfurt, Germany*

[74]*Joint Institute for Nuclear Research (JINR), Dubna, Russia*

[75]*Korea Institute of Science and Technology Information, Daejeon, Republic of Korea*

[76]*KTO Karatay University, Konya, Turkey*

[77]*Laboratoire de Physique Subatomique et de Cosmologie, Université Grenoble-Alpes, CNRS-IN2P3, Grenoble, France*

[78]*Lawrence Berkeley National Laboratory, Berkeley, California, USA*

[79]*Lund University Department of Physics, Division of Particle Physics, Lund, Sweden*

[80]*Nagasaki Institute of Applied Science, Nagasaki, Japan*

[81]*Nara Women s University (NWU), Nara, Japan*

[82]*National and Kapodistrian University of Athens, School of Science, Department of Physics, Athens, Greece*

[83]*National Centre for Nuclear Research, Warsaw, Poland*

[84]*National Institute of Science Education and Research, Homi Bhabha National Institute, Jatni, India*

[85]*National Nuclear Research Center, Baku, Azerbaijan*

[86]*National Research Centre Kurchatov Institute, Moscow, Russia*

[87]*Niels Bohr Institute, University of Copenhagen, Copenhagen, Denmark*

[88]*Nikhef, National institute for subatomic physics, Amsterdam, Netherlands*

[89]*NRC Kurchatov Institute IHEP, Protvino, Russia*

[90]*NRC Kurchatov Institute ITEP, Moscow, Russia*

[91]*NRNU Moscow Engineering Physics Institute, Moscow, Russia*

[92]*Nuclear Physics Group, STFC Daresbury Laboratory, Daresbury, United Kingdom*

[93]*Nuclear Physics Institute of the Czech Academy of Sciences, Řež u Prahy, Czech Republic*

[94]*Oak Ridge National Laboratory, Oak Ridge, Tennessee, USA*

[95]*Ohio State University, Columbus, Ohio, USA*

[96]*Petersburg Nuclear Physics Institute, Gatchina, Russia*

[97]*Physics Department, Faculty of Science, University of Zagreb, Zagreb, Croatia*

[98]*Physics Department, Panjab University, Chandigarh, India*

[99]*Physics Department, University of Jammu, Jammu, India*

[100]*Physics Department, University of Rajasthan, Jaipur, India*

[101]*Physikalisches Institut, Eberhard-Karls-Universität Tübingen, Tübingen, Germany*

[102]*Physikalisches Institut, Ruprecht-Karls-Universität Heidelberg, Heidelberg, Germany*

[103]*Physik Department, Technische Universität München, Munich, Germany*

[104]*Politecnico di Bari, Bari, Italy*

[105]*Research Division and ExtreMe Matter Institute EMMI, GSI Helmholtzzentrum für Schwerionenforschung GmbH, Darmstadt, Germany*

[106]*Rudjer Bošković Institute, Zagreb, Croatia*

[107]*Russian Federal Nuclear Center (VNIIEF), Sarov, Russia*

[108]*Saha Institute of Nuclear Physics, Homi Bhabha National Institute, Kolkata, India*

[109]*School of Physics and Astronomy, University of Birmingham, Birmingham, United Kingdom*

[110]*Sección Física, Departamento de Ciencias, Pontificia Universidad Católica del Perú, Lima, Peru*

[111]*Shanghai Institute of Applied Physics, Shanghai, China*

[112]*St. Petersburg State University, St. Petersburg, Russia*

[113]*Stefan Meyer Institut für Subatomare Physik (SMI), Vienna, Austria*

[114]*SUBATECH, IMT Atlantique, Université de Nantes, CNRS-IN2P3, Nantes, France*

[115]*Suranaree University of Technology, Nakhon Ratchasima, Thailand*

[116]*Technical University of Košice, Košice, Slovakia*

[117]*Technische Universität München, Excellence Cluster 'Universe , Munich, Germany*

[118]*The Henryk Niewodniczanski Institute of Nuclear Physics, Polish Academy of Sciences, Cracow, Poland*

[119]*The University of Texas at Austin, Austin, Texas, USA*

[120]*Universidad Autónoma de Sinaloa, Culiacán, Mexico*

[121]*Universidade de São Paulo (USP), São Paulo, Brazil*

[122]*Universidade Estadual de Campinas (UNICAMP), Campinas, Brazil*

[123]*Universidade Federal do ABC, Santo Andre, Brazil*

[124]*University of Cape Town, Cape Town, South Africa*

[125]*University of Houston, Houston, Texas, USA*

[126]*University of Jyväskylä, Jyväskylä, Finland*

[127]*University of Liverpool, Liverpool, United Kingdom*

[128]*University of Science and Techonology of China, Hefei, China*

[129]*University of South-Eastern Norway, Tonsberg, Norway*

[130]*University of Tennessee, Knoxville, Tennessee, USA*

[131]*University of the Witwatersrand, Johannesburg, South Africa*

[132]*University of Tokyo, Tokyo, Japan*

[133]*University of Tsukuba, Tsukuba, Japan*

[134]*Université Clermont Auvergne, CNRS/IN2P3, LPC, Clermont-Ferrand, France*

[135]*Université de Lyon, Université Lyon 1, CNRS/IN2P3, IPN-Lyon, Villeurbanne, Lyon, France*

[136]*Université de Strasbourg, CNRS, IPHC UMR 7178, F-67000 Strasbourg, France, Strasbourg, France*

[137]*Université Paris-Saclay Centre d Etudes de Saclay (CEA), IRFU, Département de Physique Nucléaire (DPhN), Saclay, France*

[138]*Università degli Studi di Foggia, Foggia, Italy*

[139]*Università degli Studi di Pavia, Pavia, Italy*

[140]*Università di Brescia, Brescia, Italy*

[141]*Variable Energy Cyclotron Centre, Homi Bhabha National Institute, Kolkata, India*

[142]*Warsaw University of Technology, Warsaw, Poland*

[143]*Wayne State University, Detroit, Michigan, USA*

[144]*Westfälische Wilhelms-Universität Münster, Institut für Kernphysik, Münster, Germany*

[145]*Wigner Research Centre for Physics, Hungarian Academy of Sciences, Budapest, Hungary*
[146]*Yale University, New Haven, Connecticut, USA*
[147]*Yonsei University, Seoul, Republic of Korea*

[a]Dipartimento DET del Politecnico di Torino, Turin, Italy.
[b]M.V. Lomonosov Moscow State University, D.V. Skobeltsyn Institute of Nuclear, Physics, Moscow, Russia.
[c]Deceased.
[d]Department of Applied Physics, Aligarh Muslim University, Aligarh, India.
[e]Institute of Theoretical Physics, University of Wroclaw, Poland.